INFLUENCE OF Ce ION IMPLANTATION ON OXIDATION BEHAVIOR OF Ni20Cr ALLOY①

Li Meishuan, Ma Xinqing, Xi Lio, Li Tiefan
State Key Laboratory for Corrosion and Protection, Institute of Corrosion and Protection of Metals, Chinese Academy of Sciences, Shenyang 110015

ABSTRACT The ion implantation of 2×10^{16}, 5×10^{16} and 1×10^{17} Ce^+/cm^2 to Ni20Cr alloy can significantly decrease its oxidation rate at 1000 ℃ and 1100 ℃, and improve the adhesion of oxide scales. The influence of Ce ion implantation on the binding energy of alloying elements has been studied by Ion Microprobe Miss Analyzer (IMMA). The binding energy of Cr^+ in the implanted layer of the alloy decreases, which promotes the protective Cr_2O_3 to form quickly during the initial oxidation stage. However the binding energies of Cr^+ and Ni^+ in the oxide scales increase, and the outward diffusion of Cr^{3+} and Ni^{2+} through the oxide scales is suppressed. This result may be related to changing the concentration of defects due to Ce ion implantation. After cyclic oxidation at 1000 ℃ for 270 times, the beneficial effect of Ce on the resistance to oxidation is still obvious.

Kev words oxidation cerium Ni20Cr alloy ion implantation

1 INTRODUCTION

It is well known that the addition of rare earth (RE) elements to alloys can enhance the protective properties of chromia scales. Many hypotheses have been advanced to explain this so-called RE effect[1-3]. However, this problem has not yet been solved thoroughly so far. Recently, much work has been done about the oxidation behavior of alloys modified by the addition of these RE elements by ion implantation, and significant progress has been made[4-6]. However, most work is in focus on the RE effect based on diffusion of alloying elements through the oxide grain boundaries. In this condition, RE segregates in the oxide grain boundaries, and retards the diffusion of alloying elements. At higher temperatures, the diffusion of alloying elements through oxide lattice also plays an unnegligible role in the oxidation of alloys. In general, their diffusion coefficients (D_{app}) equal the total of the lattice diffusion coefficients (D_L) and the grain boundary diffusion coefficients (D_g), i. e. $D_{app}=(1-f)D_L+fD_g$, in which f is a factor relating to the size of the grain and the width of the grain boundary. The influence of RE on the diffusion of cations through the lattice of oxide grain also needs paying more attention. In the present study, the isothermal and cyclic oxidation of cerium implanted Ni20Cr alloy has been studied at 1000 ℃ and 1100 ℃. Especially, the ion microprobe analysis technique has been used to demonstrate the influence of cerium implantation on the binding energy of alloying elements before and after oxidation. The mechanism through which implanted RE ions affect has been discussed.

2 EXPERIMENTAL PROCEDURE

All specimens were cut to dimensions of 20 mm × 10 mm × 2 mm from cast Ni20Cr ingot, polished with 800 grit SiC paper, cleaned ultrasonically in acetone, and then implanted with cerium. Three different doses of 2×10^{16}, 5×10^{16} and 1×10^{17} cerium ions cm^{-2} were applied.

① Supported by the National Natural Science Foundation of China Received Jan. 15, 1997; accepted Apr. 15, 1997

During the implantation, a voltage of 45keV and a beam of 1.8mA were maintained.

The isothermal oxidation at 1 000 ℃ and 1 100 ℃and cyclic oxidation at 1000 ℃ were carried out in air. The change of the binding energy of alloying elements due to cerium implantation was evaluated using LT-1A type of Ion Microprobe Mass Analyzer (IMMA).

3 RESULTS

3.1 Oxidation kinetics

The oxidation kinetics of the plain Ni20Cr alloy and the Ce-implanted ones at 1 000 ℃ and 1 100 ℃ are shown in Fig. 1. The kinetic curves are nearly parabolic.

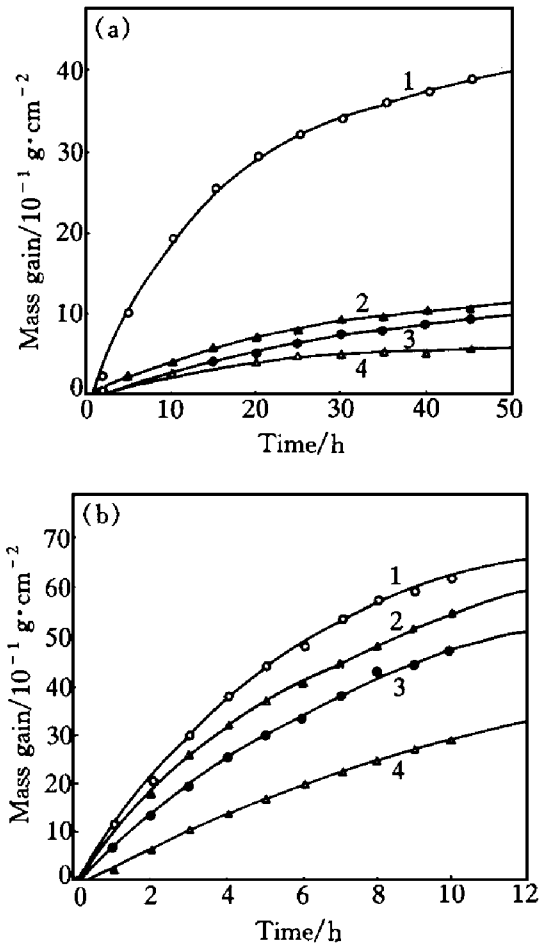

Fig. 1 Oxidation kinetics of plain and Ce-implanted Ni20Cr alloys in air at 1 000 ℃ (a) and 1 100 ℃ (b)

1—Ni20Cr; 2—Ni20Cr+ 2×10^{16} Ce^+/cm^2; 3—Ni2Cr+ $5\times10^{16}Ce^+/cm^2$; 4—Ni20Cr+ $1\times10^{17}Ce^+/cm^2$

Fig. 2 shows the cyclic oxidation kinetics of specimens at 1 000 ℃ in air. The cyclic condition is 1 h at 1 000 ℃ in furnace and 10 minutes cooling in ambient temperature air.

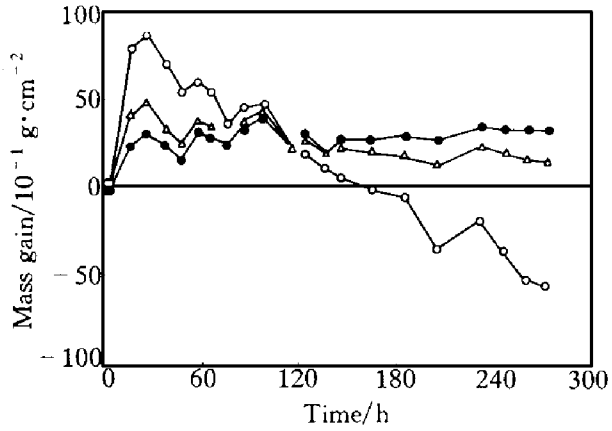

Fig. 2 Cyclic oxidation of plain and Ce-implanted Ni20Cr alloys at 1 000 ℃ in air

(Cyclic condition: 1 h at 1 000 ℃, 10 min in ambient air)

○—Ni20Cr; △—Ni20Cr+ 2×10^{16} Ce^+/cm^2; ●—Ni20Cr+ $1\times10^{17}Ce^+/cm^2$

3.2 Evaluation of binding energy difference

The variance of the binding energy of Cr^+ in the alloy surface layer and that of Cr^+ and Ni^+ in the oxide scales due to Ce implantation have been studied by IMMA. Based on the consideration of total energy for the ion bumping one time (in this condition, the secondary ion has the maximum kinetic energy), the following equation can be obtained[7-9]:

$$E_P = E_k + E_b + E_l \quad (1)$$

where E_P is the kinetic energy of primary ion beam, E_k is the kinetic energy of secondary ion beam, E_b is the binding energy, and E_l is the sum of energy losses. In the test, E_P is maintained invariably, and E_l can be treated as a constant. If the binding energy of an alloying element may change after implantation, the binding energy difference equals:

$$\Delta E_b = -\Delta E_k = -e\Delta V_R$$

(for one valence cation) (2)

Therefore, the lower the kinetic energy of the sputtered particle, the higher the binding energy of the atom in the lattice.

A grid (the grid voltage is + 1 450 V) was

connected between the receiving slit and the transfer electrode of LT-1A type IMMA. The grid voltage (or retarding voltage V_R) was changed continually from the lowest to the highest, and the secondary ion intensity I was recorded. When I equals zero, the difference of the maximum cut-off voltage and then ΔE_b can be gained. Generally, the value of V_R is determined by the cross point between the tangent line of the I-V_R curve and the X-axis[7].

The obtained testing data are shown in Fig. 3. In the test, the source of the primary ion beam is Ar^+, the accelerate voltage is 14.5 kV, the beam intensity is 0.5 μA, and the diameter of ion beam is 80 μm. From Fig. 3, the data for ΔE_b (namely, $E_b - E_{b,RE}$) are gotten, and listed as follows: (a) ΔE_b= 11keV, (b) ΔE_b= 27keV, and (c) ΔE_b= 14keV. The values of atom binding energy normally are in the order of several hundreds[10]. Therefore, the binding energy decreases about two percent after cerium ion implantation in this work.

3.3 Oxide morphologies and Ce distribution

XRD analysis indicates that, $NiCr_2O_4$ and Cr_2O_3 are formed on all the specimens isothermally oxidized. However, besides $NiCr_2O_4$ and Cr_2O_3, NiO is also found on Ni20Cr alloy oxidized cyclically. The surface morphologies of the oxide scales formed due to isothermal oxidation are presented in Fig. 4.

The Ce distribution has been determined by IMMA (see Fig. 5). The oxide/alloy interface was defined by the measurement for the concentration of Cr and Ni. Their concentrations changed noticeably at the oxide/alloy interface. On the contrary to the isothermal oxidation, the oxide scales of Ce-implanted Ni20Cr alloy spall off repeatly during cyclic oxidation, a portion of the implanted cerium has been lost, so that the total content of Ce in the scale is low.

4 DISCUSSION

The cerium implantation with three different doses obviously reduces the oxidation rate of Ni20Cr alloy at 1000 ℃ and 1100 ℃. The higher the dose of Ce implantation, the more obvious the effect of cerium. The scales spalled off during cyclic oxidation at 1000 ℃, however, the mass gain still maintained positive for Ce-implanted alloys after 270 h. After the isothermal oxidation at 1100 ℃ for 12 h, only the oxide scale formed on unimplanted Ni20Cr alloy spalled off, and those formed on implanted Ni20Cr alloys adhere tightly. Therefore, the cerium implantation may also enhance the adherence of the oxide scales.

In the early stages of oxidation of Ni20Cr alloy, the outward diffusion of Cr^{3+} cations predominates, and Cr_2O_3 is formed preferentially on the surface of the alloy[2, 3]. After that, due to the depletion of Cr in the out layer of the alloy, Ni ions begin to diffuse outward. After NiO is

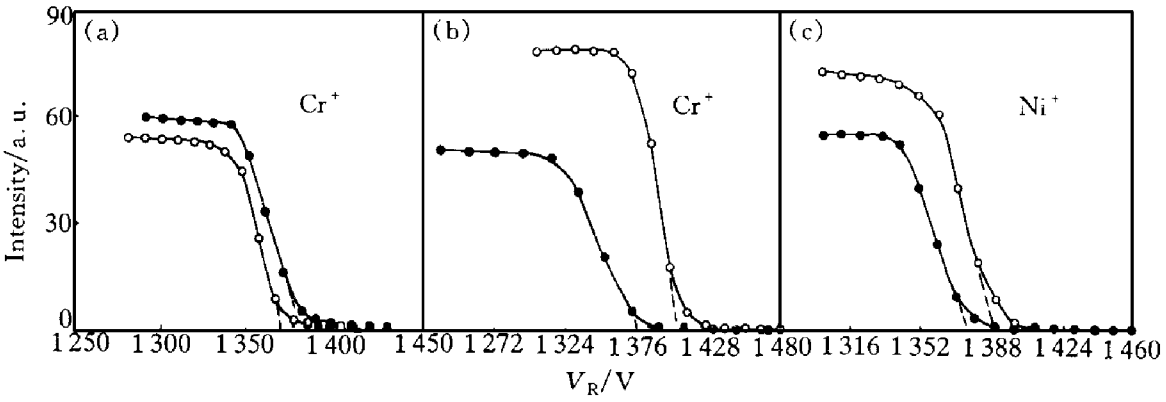

Fig. 3 Secondary ion intensity vs retarding potential for Cr^+ and Ni^+

○—Ni20Cr, ●—Ni20Cr+ 1×10^{17} Ce^+/cm^2

(a) —on surface of Ce-implanted Ni20Cr; (b), (c) —in oxide scales formed at 1100 ℃ for 12 h

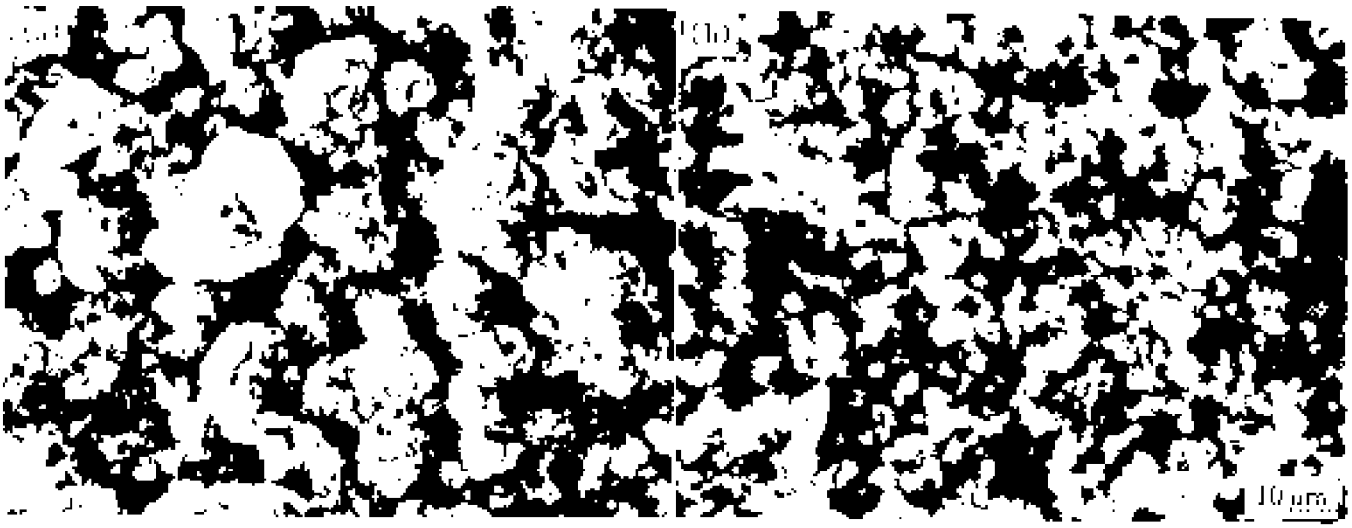

Fig. 4 Surface morphologies of oxide scales after oxidation at 1 100 ℃ for 12 h
(a) —Ni20Cr; (b) —Ni20Cr+ $1 \times 10^{17} Ce^+ / cm^2$

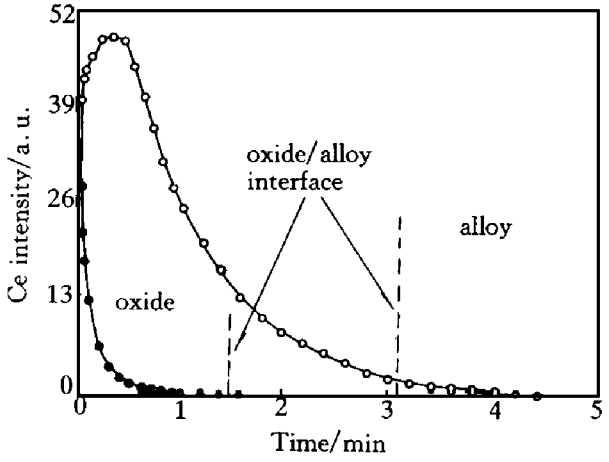

Fig. 5 Ce concentration measured by IMMA
○—Ni20Cr+ 1×10^{17} Ce^+ / cm^2, isothermal oxidation at 1 000 ℃;
●—Ni20Cr+ $1 \times 10^{17} Ce^+ / cm^2$, cyclic oxidation at 1 000 ℃

formed, it reacts with Cr_2O_3 to develop $NiCr_2O_4$. It was demonstrated by STEM that yttrium cations segregate to the boundaries of Cr_2O_3 grains formed on Co-Cr alloys[5, 6], and retard the outward diffusion of cations, leading to decreasing the oxidation rate. Furthermore, the high concentration of yttrium cations segregating at the boundaries may cause the grain size of the oxide to decrease[5, 6]. For the alloy forming Cr_2O_3 after oxidation, this result is quite general[2]. In this work, it was also found that the grain size of the oxide formed on 1×10^{17} Ce^+ / cm^2 implanted Ni20Cr alloy is much smaller than that of the oxide formed on unimplanted Ni20Cr alloy (see Fig. 4), but the implantation of 2×10^{16} Ce^+ / cm^2 has little influence on the oxide grain size. It can be seen from Fig. 5 that, the peak of the concentration of cerium is located in the outer layer of the oxide after the oxidation at 1 000 ℃ (The thickness of the implantation layer is only in the order of a few hundreds Angstroms). Therefore, the new oxide is mainly formed near the oxide/alloy interface, and the inward diffusion of O^{2-} anions predominates during the oxidation of Ce-implanted Ni20Cr alloy.

Based on Eqn. (2) and the test results in Fig. 3, the binding energy of Cr^+ decreased after implantation. However, the binding energy of Cr^+ and Ni^+ in the oxide scale increased obviously (The test was carried out on the oxide surface in Fig. 3, but the result obtained within the oxide scale is the same.). Because the diameter of primary ion beam is 80 μm, the test result can represent the real value in the oxide grain. Cerium implantation has an influence on the binding energy of alloying elements in the surface layer of the alloy or in the oxide scale. It can be thought that this result is related to the influence of cerium on the concentration of defects. The implantation is a technique for materials modification by which high energy ions are put into materials directly. The implantation also results in the development of defects in materials.

Therefore, the binding energy of Cr^+ on the surface of Ce-implanted Ni20Cr alloy decreases. On the contrary, the ion radius of rare earth elements is bigger than that of general alloying elements. These RE ions can serve as the sources of vacancy sinking[1-3]. Therefore, the concentration of the vacancies in the oxide grains decreases, while the binding energy of alloying elements is increased.

The binding energy of Cr^+ decreased after implantation. This means that the cerium implantation is beneficial to the outward diffusion of Cr^+ cations, and promotes the quick formation of the protective Cr_2O_3 scale in the initial oxidation stage. However, the binding energy of Cr^+ and Ni^+ in the oxide increased, and the outward diffusion of the cations through the grain lattice is retarded. In a word, when the Ni20Cr alloy is oxidized at 1 000 ℃ and 1 100 ℃, because of being retarded for the outward diffusion of cations through the oxide grain boundary and oxide lattice, the oxidation rates of the Ce-implanted alloys decrease.

$NiCr_2O_4$ and Cr_2O_3 are mainly developed during the oxidation of Ni20Cr alloy. The surface investigation indicates that the oxide scales formed on Ce-implanted Ni20Cr alloys are compact and entire. The outward diffusions of Cr^+ and Ni^+ are retarded, and the segregation of a great number of vacancies at the interface is avoided. Thus, the adhesion of the oxide scale to the alloy is enhanced. On the other hand, the residual stresses in the oxide scales have been measured by Laser Roman Spectroscopy. The result indicates that the residual stress in the oxide scale of Ce-implanted Ni20Cr alloy is smaller. Due to the reasons mentioned above, cerium implantation can improve the adhesion of the oxide scale.

Because the thickness of the implantation layer is in the order of hundreds Angstroms, if the oxide scale is thick or happens to spall many times, the content of cerium decreases. Finally, the beneficial effect of cerium on the oxidation resistance of Ni20Cr may disappear. However, it can be seen from Fig. 2 that, although the cyclic times get to 270, the effect of cerium is still marked.

5 CONCLUSIONS

(1) The implantation of 2×10^{16}, 5×10^{16}, 1×10^{17} cerium ions cm^{-2} to Ni20Cr alloy can reduce the oxidation rate at 1 000 ℃ and 1 100 ℃, and improve the adherence of the oxide scales.

(2) The binding energy of Cr^+ in the surface layer decreases, however, those of Cr^+ and Ni^+ in the oxide scale increase. This result can be accounted for the influence of implantation of cerium on the defect concentration.

(3) After cyclic oxidation at 1 000 ℃ for 270 times, the beneficial effect of implanted cerium on the oxidation resistance is still marked.

REFERENCES

1 Hindam H, Whittle D P. Oxid Metals, 1982, 18: 245-284.
2 Moon D P. Mater Sci Technol, 1989, 5: 754-764.
3 Stringer J. Mater Sci Eng, 1989, A120: 129.
4 Stott F H, Punni J S *et al*. Ion Implantation Into Metals. New York: Pergamon Press, 1982: 245-254.
5 Przybylski K, Garratt-Reed A J, Yurek G J. J Electrochem Soc, 1988, 135: 509-517.
6 Cotell C M, Yurek G J *et al*. Oxid Metals, 1990, 34: 173-216.
7 Wan X, Yang K, Cao M. Acta Metallurgica Sinica, 1986, 22: A189-A194.
8 Chen L, Liu S, Zhou J *et al*. Chinese J Mass Spectrum, (in Chinese), 1988, 9: 32.
9 Gao P. In: Proc of 8th International Congress on Metallic Corrosion, Mainz, Germany, 1981, 1: 406-413.
10 Abderrazik G B, Moulin G, Huntz A M. Oxid Metals, 1990, 33: 191-236.

(Eidted by He Xuefeng)